

Fig. 1 Schematic of rf gas discharge volume.

Figure 1 shows a design of a water-cooled copper discharge volume. The jacket is formed from a single piece of copper sheet (0.035 in.) and contains a divider opposite the slit; thus, each half of the jacket is separately cooled. All joints are silver soldered for low electrical resistance and for high strength. Cooling water at about 500 psi is pumped through the water jacket in order to insure adequate cooling of the copper wall; the annular cooling passage gap is about 0.035 in. The first turn of the copper solenoid ($\frac{3}{16}$ -in. tubing) is shorted to the jacket's outer wall, and the remainder of the turns are embedded in a Teflon sleeve containing a $\frac{3}{16}$ -in. machined spiral in its outside surface; the Teflon prevents arcing between adjacent coils and between the coil and the jacket walls. The slit in the water jacket is sealed with boron nitride, a high temperature electrical insulator, which is carefully machined to fit the slit. The boron nitride separator is made gas tight by sealing both outer edges which are in contact with the cold outer jacket wall with high temperature Sauereisen cement. The mica disk on the bottom of the jacket shields the Teflon sleeve from any free convective flow of heated gas.

The gas is injected with a tangential component of motion through three critical flow orifices into the discharge volume. The tangential injection provides a swirling motion to the heated gas which tends to stabilize the discharge; the critical flow condition allows simple metering of the gas mass flow rate by measuring only the injection manifold pressure. The gas injection assembly is separated from the discharge volume by about 10 in. of connecting glass tube. This separation is necessary in order that the gas injection assembly does not act as an electrode causing an "E" type discharge and thereby absorbing some of the incident power.

Figure 2 shows the copper water-jacketed discharge volume in operation. An argon plasma having an enthalpy of about 100 kcal/gm-mole is being generated which discharges to atmospheric pressure. The enthalpy at atmospheric pressure corresponds to an equilibrium gas temperature of about 12,000°K. This water jacket design has been operated at this enthalpy level for times of an hour with no noticeable wall erosion.

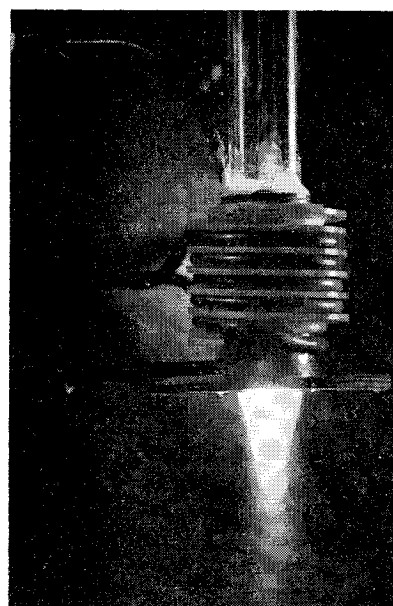


Fig. 2 Argon plasma, 100 kcal/g-mole at 1 atm.

References

- 1 Mironer, A. and Hushfar, F., "Radio frequency heating of a dense moving plasma," AIAA Preprint 63045-63 (March 1963).
- 2 Reed, T. B., "Induction-coupled plasma torch," J. Appl. Phys. 32, 821-824 (May 1961).
- 3 Cannon, H. R., "A study of an induction-coupled plasma operating at 400 kilocycles," MS Thesis, Air Force Institute of Technology (August 1962).

Coning Effects Caused by Separation of Spin-Stabilized Stages

M. DWORK*

Airborne Instruments Laboratory, † Deer Park, N. Y.

Nomenclature

I_L = longitudinal moment of inertia of body
 I_T = transverse moment of inertia of body
 \bar{M} = total momentum vector
 M_L = longitudinal momentum
 M_T = transverse momentum
 m = mass of body
 μ = reduced mass of configuration = $m_1 m_2 / (m_1 + m_2)$
 l = separation between center of masses of body 1 and body 2 prior to separation
 ω_L = longitudinal angular speed
 ω_T = transverse angular speed
 θ = coning angle = $\tan^{-1}(M_T / M_L)$

Subscripts

1 = body 1, payload
2 = body 2, booster

FOR spin-stabilized booster-payload configurations that are coning, it has been observed that the coning angle of the payload after separation is appreciably different from that of the combination. At first, it seems logical to blame the separation mechanism for introducing a tip-off condition. However, it is physically possible for the coning angle to change even with a perfect separation mechanism. As shown

Received June 6, 1963.

* Consultant, Advanced Projects Department. Member AIAA.
† A division of Cutler-Hammer.

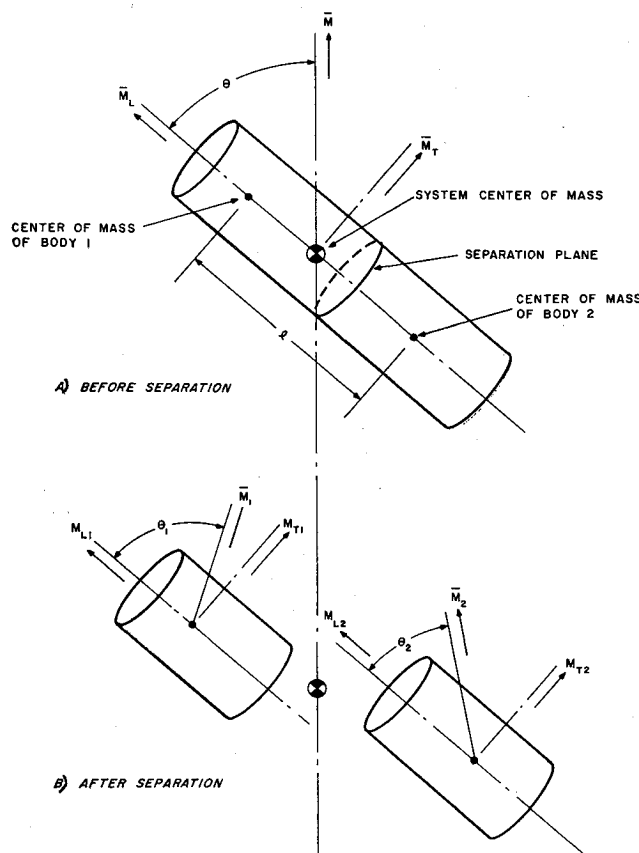


Fig. 1 Vector diagram.

in Fig. 1, the angular momentums about the longitudinal and transverse axes prior to separation are

$$M_L = (I_{L_1} + I_{L_2} + \mu l^2) \omega_1 \quad (1)$$

$$M_T = (I_{T_1} + I_{T_2}) \omega_1 \quad (2)$$

The coning angle is defined as

$$\tan \theta = \frac{M_T}{M_L} = \left(\frac{I_{T_1} + I_{T_2}}{I_{L_1} + I_{L_2} + \mu l^2} \right) \frac{W_1}{W_1} \quad (3)$$

Immediately after separation and assuming a perfect separation mechanism, the components of angular momentum of m_1 about its own center of mass are

$$M_{L_1} = I_{L_1} \omega_{1i} \quad (4)$$

$$M_{T_1} = I_{T_1} \omega_{1i} \quad (5)$$

But $\omega_{1i} = \omega_1$ and $\omega_{1i} = \omega_2$, since in the process of separation no external torques were introduced. The coning angle for m_1 is

$$\tan \theta_1 = I_{T_1} \omega_1 / I_{L_1} \omega_1 \quad (6)$$

In a similar manner,

$$M_{L_2} = I_{L_2} \omega_{2i} \quad (7)$$

$$M_{T_2} = I_{T_2} \omega_{2i} \quad (8)$$

$$\tan \theta_2 = (I_{T_2} / I_{L_2}) (\omega_2 / \omega_1) \quad (9)$$

Angular momentum of the system is conserved by the motion of m_1 and m_2 about the system center of mass. The coning angle of the payload after separation is increased or decreased over that of the configuration before separation according to the relationship

$$\frac{I_{T_2}}{I_{L_2}} = \frac{I_{T_1} + I_{T_2}}{I_{L_1} + I_{L_2} + \mu l^2} \quad (10)$$

which can be written as

$$0 < \frac{I_{T_2}}{I_{T_1}} - \frac{I_{L_2}}{I_{L_1}} - \frac{\mu l^2}{I_{L_1}} \quad (11)$$

Similar relationships are true for the booster coning angle. It is, therefore, possible for the coning angle of the payload to increase or decrease even with a perfect separation mechanism.

Choosing Optical Properties of Noncharring Ablators

LAWRENCE E. HOOKS*

Air Force Systems Command,
Wright-Patterson Air Force Base, Ohio

Nomenclature

a	attenuation coefficient
E	σT^4
\dot{m}	mass ablation rate per unit area
q^*	ablation parameter
r	flake reflectivity
T	absolute temperature
σ	Stefan-Boltzmann constant

Subscript

A = ablation

THE noses of superorbital re-entry vehicles will receive significant radiant heating pulses during deceleration to orbital speeds. Designers of such vehicles must prevent this energy from penetrating to the load-bearing structures. This may be done by using opaque heat shields, charring ablatives, or ablatives that have opaque vapor states. Discussing transparent, noncharring ablatives with transparent vapor states, Allen¹ suggests another way to prevent radiation penetration: add metal flakes to the heat shield, orienting these flakes to reflect gas cap radiation away from the vehicle.

This note develops the ablation rate expression for a transparent ablator and simplifies the expression for two conditions: negligible radiant heating and substantial radiant heating. The transparent ablator is compared to an opaque ablator on the basis of minimum ablation rate for the two radiant heating conditions.

Assuming that the first metal flakes in the transparent ablator are located parallel to the shield surface at a depth L and that thermal conduction is negligible in the surface layer of depth L (L layer), the power balance for an elemental area of the L layer and the flake may be written as

$$q_{ei} + q_{Ri} = q_A + q_e + q_{R0} \quad (1)$$

where q_{ei} is convective heat flux in, q_{Ri} is flux in due to gas cap radiation, q_A is flux carried away by vaporized ablator, q_e is thermal emission from the L layer and the flake, and q_{R0} is unabsorbed gas cap radiation leaving the area element after reflection from the flake.

The net heating into the skin element is

$$q_{Ni} = q_{ei} + q_{NR} = q_A + q_e \quad (2)$$

where $q_{NR} \equiv q_{Ri} - q_{R0}$ is the net radiant energy absorbed by the L layer and the flake. Now,

$$q_A = q^* \dot{m} \quad (3)$$

Received June 13, 1963; revision received August 19, 1963. The author thanks W. L. Hankey Jr. for his aid during preparation of this note.

* Physicist, Air Force Flight Dynamics Laboratory, Research and Technology Division.